ISSN 1330-3651 (Print), ISSN 1848-6339 (Online)
https://doi.org/10.17559/TV-20190423010908
Original scientific paper

The Effect of the Co-Planar Structure on HPBW and the Directional Gain at the Square Patch Antenna around ISM 2450 MHz

Orhan ARMAGAN*, Mesud KAHRIMAN

Abstract: In this study, ISM-band microstrip square patch antenna with 2450 MHz operating frequency was designed, the S11 reflection coefficient of the antenna and the maximum antenna gain at φ and θ angles was determined, and the values of HPBW were calculated. The simulations were performed in Ansoft HFSS and the accuracy of the gain value enhancement in the results was confirmed by CST Studio Suit. Then, by placing the co-planar structure around this patch, the values for different co-planar thicknesses were obtained again. The maximum antenna gain of the co-planar structure in φ and θ angles and its effect on HPBW values were compared. According to this, the maximum gain value of 113 × 118 mm microstrip square patch antenna with no co-planar structure was obtained as 0,308 dB and HPBW value was obtained as 55,05°. When these values were obtained again by adding co-planar structure without changing the antenna dimensions, it was observed that the maximum gain value was 0,748 dB and HPBW value was 49,46°. As can be understood from these values, the addition of co-planar structure was observed to have a positive effect on the antenna parameters by causing the increase in Maximum Gain. HPBW values decreased contrast to the gain. Here, it was observed that adding co-planar structure increased the directionality and max gain of the antenna on the radiation pattern, and the θ angle, in which the max gain occurred, shifted from 90 to 85. It was also observed that a similar effect occurred at different antenna sizes. Traditionally, antenna gain is achieved by increasing antenna dimensions. In this study, it was investigated to increase the antenna gain without increasing the antenna size marginally.

Keywords: 2450 MHz; co-planar; gain; HPBW; ISM; microstrip antenna; patch antenna

1 INTRODUCTION

The idea that microstrip structures were an emitter element making radiation and that they could be used as an antenna was first proposed by Deschamps in 1953. Related to this issue, the first patent was obtained in 1955 by Gutton and Baissinot in France. Different antenna recommendations, in which co-planar structure is added to the patch antenna, are available in the literature.

In their study conducted to improve bandwidth, Cui and his colleagues placed a U-shaped slot on each leaf of the four-leaf clover. While they obtained 67% bandwidth around the reflection coefficient under –15 dB, they developed an eight-element antenna for base station applications, and they achieved an average of 17dBi gain and 65 ± 5° HPBW [1]. Omar et al. have used CPW in a sawtooth-like circular patch antenna design. They obtained a UBW antenna operating in the 3,1-10,6 GHz frequency range [2]. In another study, the procedure for simultaneously improving the gain, bandwidth and efficiency of a microstrip patch antenna is presented [3]. Dardeer et al. designed a simple planar quad-band rectangular monopole antenna with dual E-shaped stubs for GSM/WLAN/WiMAX and they used CPW feed in this antenna [4]. Barrou et al. performed a performance comparison study on the gain and HPBW parameters of microstrip patch antennas with conventional geometries. [5]. Different techniques have been investigated to reduce antenna dimensions [6]. There are also studies focusing on co-planar structured array antenna and using the CPW feeding [7-11]. In addition, there are different studies on the improvement of s parameters [12] , bandwidth [11, 13, 14] and gain [14-18].

In this study, the effect of adding coplanar structure to a microstrip square patch antenna without changing antenna dimensions on antenna gain and HPBW are presented.

In this section, the studies in the literature have been mentioned and in the 2nd section, information related to the Antenna Radiation Pattern and Half Power Beam Width is given and information about the antenna used in the study is presented. In the 3rd section, the simulation results obtained from the antennas are shown in tables and graphs under three different sub-headings. Finally, in section 4, the results are discussed, and the importance of the study is emphasized.

2 MATERIAL METHOD

2.1 Fundamental Equations for Rectangular Patch Antenna

Physical and effective lengths of Rectangular Microstrip Patch Antenna are shown in Fig. 1. Various formulas that can be used to design a microstrip patch antenna are written below [19].

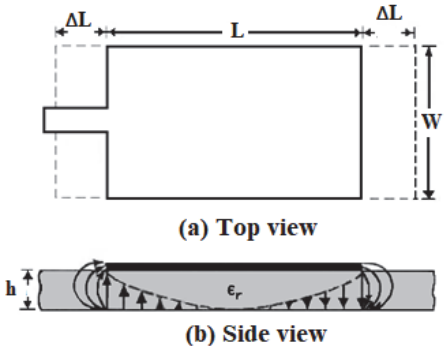

Figure 1 Physical and effective lengths of rectangular microstrip patch antenna: a) Top view; b) Side view

$$\varepsilon_{reff} = \frac{(\varepsilon_r + 1)}{2} + \frac{(\varepsilon_r - 1)}{2}\sqrt{\frac{1}{1+12\frac{h}{W}}} \quad (1)$$

ε_{reff} - effective dielectric constant,

ε_r - relative dielectric constant of the substrate

h - the thickness of substrate,

W - width of the patch.

The popular and practical approach for ΔL (Elongation in L) can be calculated by Eq. (2).

$$\frac{\Delta L}{h} = 0,412 \frac{\left(\varepsilon_{\text{reff}} + 0,3\right)\left(\frac{W}{h} + 0,264\right)}{\left(\varepsilon_{\text{reff}} - 0,258\right)\left(\frac{W}{h} + 0,8\right)} \tag{2}$$

The width of the patch W is calculated by Eq. (3).

$$W = \frac{1}{2 f_{\text{r}} \sqrt{\mu_0 \varepsilon_0}} \sqrt{\frac{2}{\varepsilon_{\text{r}} + 1}} = \frac{v_0}{2 f_{\text{r}}} \sqrt{\frac{2}{\varepsilon_{\text{r}} + 1}} \tag{3}$$

where f_{r} is the resonant frequency, v_0 is the free-space velocity of light. The actual length of the patch (L) is calculated by Eq. (4).

$$L = \frac{1}{2 f_{\text{r}} \sqrt{\varepsilon_{\text{reff}}} \sqrt{\mu_0 \varepsilon_0}} - 2\Delta L = \frac{v_0}{2 f_{\text{r}} \sqrt{\varepsilon_{\text{reff}}}} - 2\Delta L \tag{4}$$

2.2 Radiation Pattern

A radiation pattern of an antenna or an antenna pattern is a mathematical expression or graphical representation of the radiation characteristics of the antenna as a function of space coordinates. Radiation patterns of antennas are obtained using field or power values [20].

- The field pattern is the linear drawing of the Electric Field (E) or Magnetic Field (H) in angular coordinates.

The power pattern is the power (that is, the square of the Amplitude of the Electric Field or Magnetic Field), or it is:

- the linear drawing in angular coordinates,
- the decibel (dB) drawing in angular coordinates.

2.2 Half Power Beam Width (HPBM)

In the Field Pattern, the angle between the places that are 0,707 times the maximum value (Fig. 2a), in the linear scale Power Pattern, the angle between the places that are 0,5 times the maximum value (Fig. 2b), and in the decibel scale power pattern, the angle between the places that are less than 3 dB of the maximum value (Fig. 2c) are taken as HPBW.

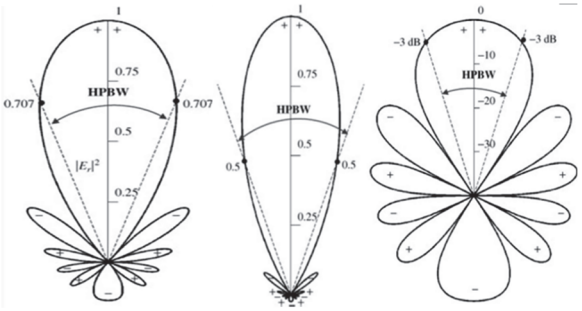

Figure 2 For HPBW calculation a) Field Pattern; b) Linear Scale Power Pattern; c) Decibel Scale Power Pattern [19]

HFSS simulation program was used for the design of Microstrip Patch Antenna. In this program, with FR4_epoxy material, the design of the microstrip square patch antenna having 2450 MHz operating frequency was made using the antenna geometry in Fig. 3.

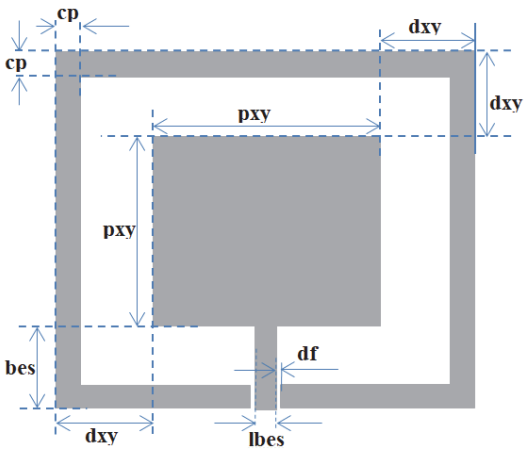

Figure 3 Geometry of the square microstrip patch antenna

There were 5 different variables in this design. By sizing these variables parametrically, 3 square patch antennas in different sizes and operating at 2450 MHz frequency were designed, and max gain and HPBW parameters were calculated for each antenna. Then, the *cp* variable was changed parametrically at 1mm intervals by adding co-planar frames to each antenna, and by calculating the Maximum Gain values in different directions and the Beam Width values, the results were turned into tables. Finally, the graphs were drawn using these values. These graphs and summary tables are presented in the 3rd section.

3 RESULTS

In this section, parametric analysis results of 3 microstrip patch antennas with different variable dimensions are presented. For simulations are used excitations port with 50 Ω characteristic impedance. In the parametric analyses, *pxy*, *lbes*, *bes* and *dxy* variables were changed parametrically, and three different analysis results for different values of *pxy, bes* and *lbes* were shown in tables and graphs.

3.1 The First Parametric Analysis Results

The 3D radiation pattern of the square patch antenna with fixed variables of *pxy* = 58 mm, *bes* = 25 mm, *lbes* = 5 mm, *dxy* = 30 mm is shown in Fig. 4. At the end of adding the co-planar frame structure, the results obtained according to the co-planar frame structure thickness variable (*cp* value) were shown in Tab. 1. Graphics are also presented in Fig. 5, Fig. 6, and Fig. 7. Fig. 8 shows the S_{11} - Frequency changing for *pxy* = 58 mm, *bes* = 25 mm, *lbes* = 5 mm, *cp* = 0 and 17 mm. Fig. 9 is the illustration of how HPBW is calculated. The θ_1 and θ_2 variables are the angles that are at the right and left of the θ_M angle and where the maximum gain falls below 3 dB. θ_M is the angle value at which the gain is maximum. The HPBW value is the difference between the θ_1 and θ_2. The *cp* variable is the co-planar structure width and *cp* = 0 is the base antenna where there is no co-planar structure.

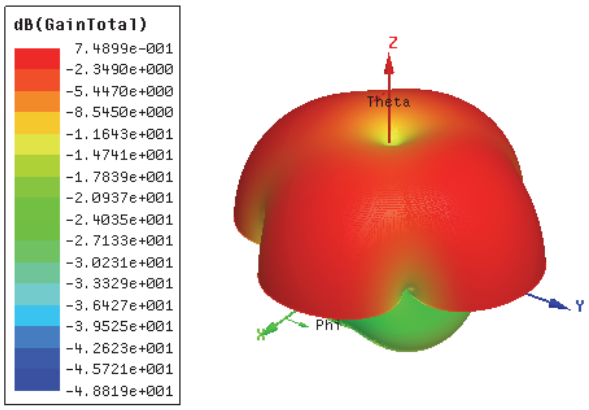

Figure 4 The 3D Radiation Pattern of the antenna which was placed on *x-y* plane and which is in dimensions of *pxy* = 58, *bes* = 25 mm, *lbes* = 5 mm, *cp* = 17 mm

Table 1 Change values of Min S_{11}, Max_Gain (dB) and HPBW according to *cp* for *pxy* = 58 mm, *bes* = 25 mm, *lbes* = 5 mm, *dxy* = 30 mm, φ = 90°, f_{GAIN} = 2,45 GHz

	$f_{c\ S11}$		Min S_{11}		GAIN		HPBW	
cp	HFSS	CST	HFSS	CST	HFSS	CST	HFSS	CST
0	2,460	2,4605	–16,43	–17,56	0,308	0,009	55,05	54,5
1	2,455	2,4565	–17,30	–26,67	–0,275	0,877	55,49	54,1
2	2,450	2,4565	–17,81	–23,26	–0,597	0,840	55,62	54,7
3	2,455	2,4565	–17,44	–21,25	–0,173	0,800	52,83	55,0
4	2,460	2,4635	–16,73	–25,65	–0,109	0,780	51,36	53,7
5	2,455	2,4595	–17,44	–26,78	–0,775	0,830	55,80	53,2
6	2,455	2,4580	–16,74	–25,43	–0,572	0,835	51,82	53,4
7	2,450	2,4575	–18,14	–24,29	–0,708	0,840	51,80	53,5
8	2,455	2,4570	–17,88	–23,08	–0,326	0,838	55,21	53,6
9	2,450	2,4575	–19,63	–22,10	–0,766	0,832	54,02	53,6
10	2,460	2,4575	–18,32	–20,77	–0,593	0,827	52,36	53,6
11	2,445	2,4575	–38,69	–19,40	–1,614	0,815	55,58	53,6
12	2,435	2,4580	–23,46	–18,07	–1,616	0,791	58,53	53,8
13	2,430	2,4575	–25,48	–16,60	–1,544	0,750	56,67	54,3
14	2,455	2,4515	–28,69	–16,24	–1,267	0,709	55,57	54,9
15	2,450	2,4495	–45,79	–17,98	0,311	0,692	51,92	55,5
16	2,455	2,4510	–28,19	–20,01	–0,126	0,702	50,56	55,7
17	2,455	2,4530	–24,02	–20,90	0,748	0,721	49,46	55,5
18	2,460	2,4545	–24,84	–21,58	–0,121	0,732	50,00	55,4
19	2,465	2,4560	–21,93	–21,98	0,063	0,737	49,80	55,3
20	2,460	2,4575	–20,07	–22,13	–0,310	0,737	51,09	55,2

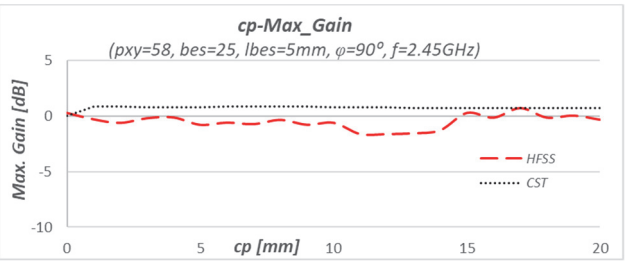

Figure 5 *cp* - Max_Gain change graph for *pxy* = 58 mm, *bes* = 25 mm, *lbes* = 5 mm, *dxy* = 30 mm, φ = 90°and *f*= 2,45 GHz

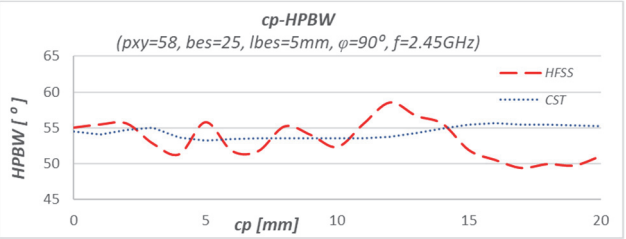

Figure 6 *cp* - HPBW change graph for *pxy* = 58 mm, *bes* = 25 mm, *lbes* = 5 mm, *dxy* = 30 mm, φ = 90° and *f* = 2,45 GHz

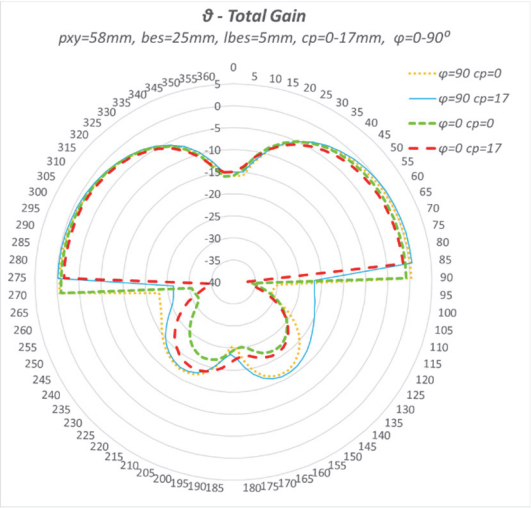

Figure 7 θ - Max_Gain (dB) Radiation Pattern graphs for *pxy* = 58 mm, *bes* = 25 mm, *lbes* = 5 mm, *dxy* = 30 mm, *cp* = 0 and 17 mm, φ = 0°and 90°, *f* = 2,45 GHz

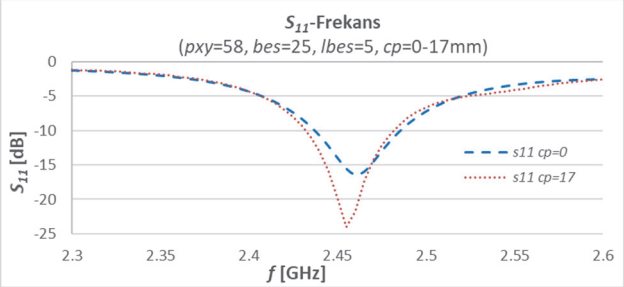

Figure 8 S_{11} - Frequency change graph for *pxy* = 58 mm, *bes* = 25 mm, *lbes* = 5 mm, *cp* = 0 and 17 mm

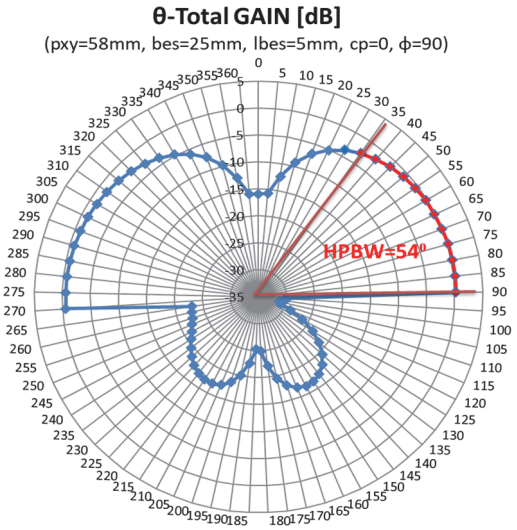

Figure 9 θ - Max_Gain Radiation Pattern graph and illustration of HPBW calculation for *pxy* = 58 mm, *bes* = 25 mm, *lbes* = 5 mm, *dxy* = 30 mm, *cp* = 0°, φ = 90°

3.2 The Second Parametric Analysis Results

The 3D radiation pattern of the square patch antenna with fixed variables of *pxy* = 58 mm, *bes* = 25 mm, *lbes* = 7 mm, *dxy* = 30 mm is shown in Fig. 10. At the end of adding the co-planar frame, the results obtained according to the frame thickness variable (*cp* value) were shown in Tab. 2. Graphics are also presented in Fig. 11, Fig. 12, Fig. 13. Fig. 14 shows the S_{11}-Frequency changing for *pxy* = 58 mm, *bes* = 25 mm, *lbes* = 7 mm, *cp* = 0 and 13 mm.

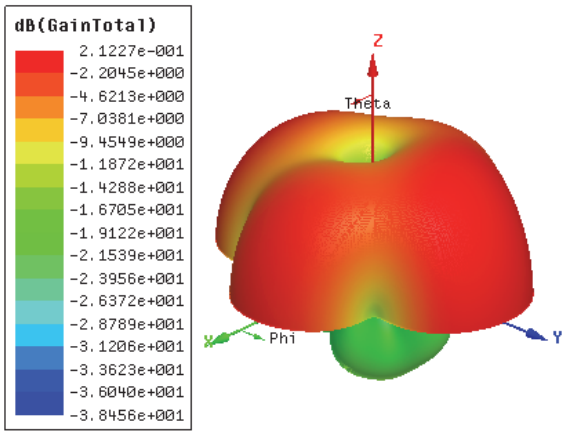

Figure 10 The 3D Radiation Pattern of the antenna which was placed on *x-y* plane, and which is in dimensions of *pxy* = 58 mm, *bes* = 25, *lbes* = 7 mm, *cp* = 13 mm

Table 2 Change values of Min S_{11}, Max_Gain (dB) and HPBW according to *cp* for *pxy* = 58 mm, *bes* = 25 mm, *lbes* = 7 mm, *dxy* = 30 mm, φ = 90°, f_{GAIN} = 2,45 GHz

	f_c		Min S_{11}		GAIN		HPBW	
cp	HFSS	CST	HFSS	CST	HFSS	CST	HFSS	CST
0	2,465	2,4720	–24,64	–24,66	0,029	–0,126	55,12	54,6
1	2,455	2,4605	–38,50	–16,70	–0,629	0,838	54,74	54,6
2	2,465	2,4605	–24,35	–15,43	–0,480	0,800	52,28	55,1
3	2,470	2,4605	–21,82	–14,59	–0,445	0,770	50,84	55,3
4	2,460	2,4690	–25,38	–15,95	–0,241	0,746	52,69	54,4
5	2,460	2,4640	–29,28	–16,85	–1,257	0,788	55,50	53,5
6	2,460	2,4630	–24,76	–16,20	–0,874	0,801	53,05	53,7
7	2,465	2,4625	–23,56	–15,83	–0,314	0,801	52,71	53,8
8	2,460	2,4615	–32,88	–15,44	–0,113	0,800	51,50	53,9
9	2,460	2,4625	–28,61	–14,97	–0,543	0,792	53,32	53,9
10	2,455	2,4625	–28,47	–14,42	–1,498	0,785	52,35	53,9
11	2,455	2,4625	–21,81	–13,80	–1,845	0,769	55,23	54,0
12	2,460	2,4630	–26,14	–13,14	–1,199	0,738	52,69	54,4
13	2,430	2,4625	–16,45	–12,42	0,211	0,698	54,41	54,9
14	2,455	2,4560	–22,47	–12,34	–0,527	0,663	52,34	55,6
15	2,460	2,4545	–28,50	–13,34	–0,103	0,654	50,78	56,1
16	2,465	2,4560	–29,12	–14,37	–0,044	0,668	49,24	56,2
17	2,465	2,4580	–29,15	–14,74	–0,356	0,686	50,53	56,1
18	2,470	2,4595	–36,19	–14,99	–0,055	0,695	49,20	55,9
19	2,470	2,4610	–30,28	–15,11	–0,755	0,699	50,05	55,8
20	2,470	2,4625	–29,92	–15,14	–0,248	0,696	48,94	55,8

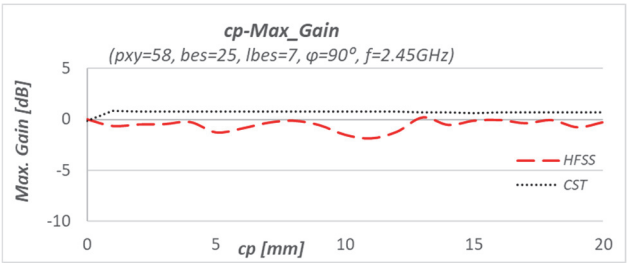

Figure 11 *cp* - Max_Gain change graph for *pxy* = 58 mm, *bes* = 25 mm, *lbes* = 7 mm, *dxy* = 30 mm and φ = 90°

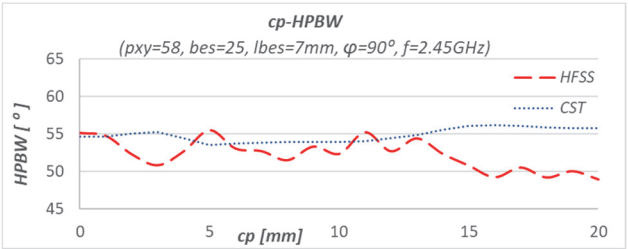

Figure 12 *cp* - HPBW change graph for *pxy* = 58 mm, *bes* = 25 mm, *lbes* = 7 mm, *dxy* = 30 mm and φ = 90°

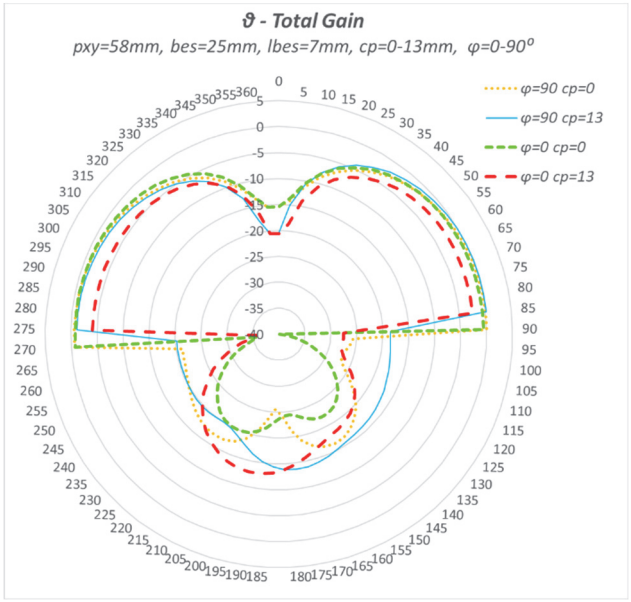

Figure 13 θ - MaxGain (dB) Radiation Pattern graphs for *pxy* = 58 mm, *bes* = 25 mm, *lbes* = 7 mm, *dxy* = 30 mm, *cp* = 0 and 13 mm, φ = 0° and 90°

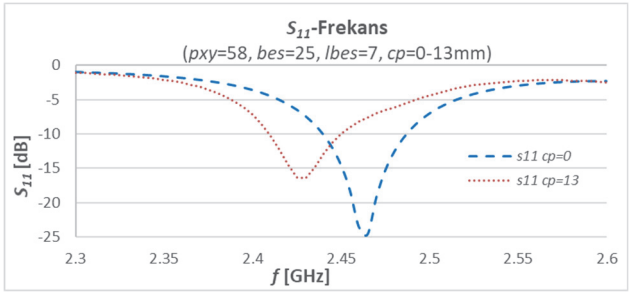

Figure 14 S_{11} - Frequency change graph for *pxy* = 58 mm, *bes* = 25 mm, *lbes* = 7 mm, *cp* = 0 and 13 mm

3.3 The Third Parametric Analysis Results

The 3D radiation pattern of the square patch antenna with fixed variables of *pxy* = 59 mm, *bes* = 20 mm, *lbes* = 8 mm, *dxy* = 30 mm is shown in Fig. 15. At the end of adding the co-planar frame, the results obtained according to the frame thickness variable (*cp* value) were shown in Tab. 3. Graphics are also presented in Fig. 16, Fig. 17, Fig. 19. Fig. 18 shows the S_{11}-Frequency changing for *pxy* = 59 mm, *bes* = 20 mm, *lbes* = 8 mm, *cp* = 0 and 14 mm.

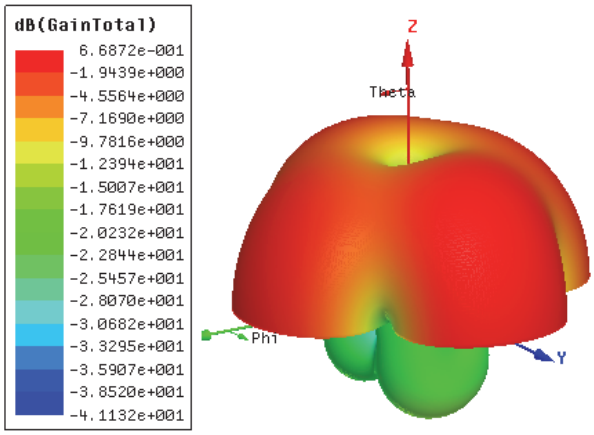

Figure 15 The 3D Radiation Pattern of the antenna which was placed on *x-y* plane and which is in dimensions of *pxy* = 59, *bes* = 20, *lbes* = 8, *cp* = 14 mm

Table 3 Change values of *Min* S_{11}, Max_Gain (dB) and HPBW according to *cp* for *pxy* = 59 mm, *bes* = 20 mm, *lbes* = 8 mm, *dxy* = 30 mm, φ = 90°, f_{GAIN} = 2,45 GHz

	f_c (for Min S_{11})		Min S_{11}		GAIN		HPBW	
cp	HFSS	CST	HFSS	CST	HFSS	CST	HFSS	CST
0	2,455	2,4625	–25,48	–35,60	0,559	–0,597	52,42	54,5
1	2,455	2,4550	–30,50	–25,18	0,279	0,799	50,29	53,8
2	2,450	2,4555	–37,89	–20,90	–0,631	0,770	52,06	54,3
3	2,450	2,4555	–26,80	–20,22	0,097	0,746	47,68	54,5
4	2,445	2,4550	–57,14	–19,18	–0,254	0,724	50,82	54,6
5	2,445	2,4590	–29,97	–17,05	0,178	0,700	51,18	54,6
6	2,450	2,4600	–31,59	–17,79	–0,750	0,691	52,03	54,4
7	2,450	2,4590	–28,69	–17,87	–0,668	0,694	52,43	54,2
8	2,450	2,4590	–35,08	–17,32	–0,534	0,693	52,66	54,3
9	2,445	2,4585	–27,30	–16,62	–1,137	0,685	53,16	54,4
10	2,455	2,4570	–40,04	–15,84	–0,310	0,675	51,36	54,6
11	2,445	2,4540	–23,55	–15,73	–0,647	0,664	52,50	54,8
12	2,460	2,4525	–40,67	–16,40	–0,083	0,653	49,87	54,9
13	2,435	2,4520	–22,64	–17,43	0,006	0,675	49,30	54,8
14	2,460	2,4520	–29,70	–18,70	0,669	0,673	50,04	54,7
15	2,460	2,4530	–30,55	–19,50	0,439	0,681	48,84	54,6
16	2,460	2,4550	–28,34	–19,82	0,494	0,690	49,40	54,5
17	2,465	2,4565	–28,50	–19,95	0,307	0,695	48,24	54,4
18	2,465	2,4585	–27,04	–19,89	0,542	0,702	47,93	54,4
19	2,460	2,4585	–22,11	–20,21	0,476	0,696	49,06	54,3

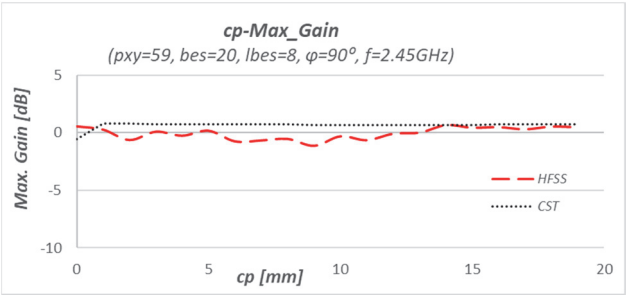

Figure 16 *cp* - Max_Gain change graph for *pxy* = 59 mm, *bes* = 20 mm, lbes = 8 mm, *dxy* = 30 mm and φ = 90°

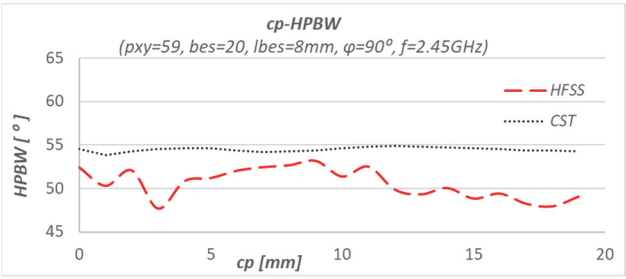

Figure 17 *cp* - HPBW change graph for *pxy* = 59 mm, *bes* = 20 mm, *lbes* = 8 mm, *dxy* = 30 mm and φ = 90°

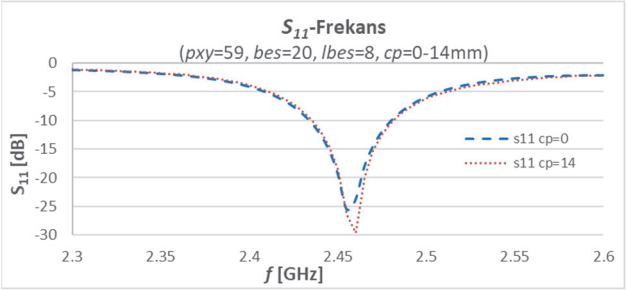

Figure 18 S_{11} - Frequency change graph for *pxy* = 59 mm, *bes* = 20 mm, *lbes* = 8 mm, *cp* = 0 and 14 mm

In the study, six different antennas with three different dimensions parameters were examined. The parameters of these antennas are given in Tab. 4.

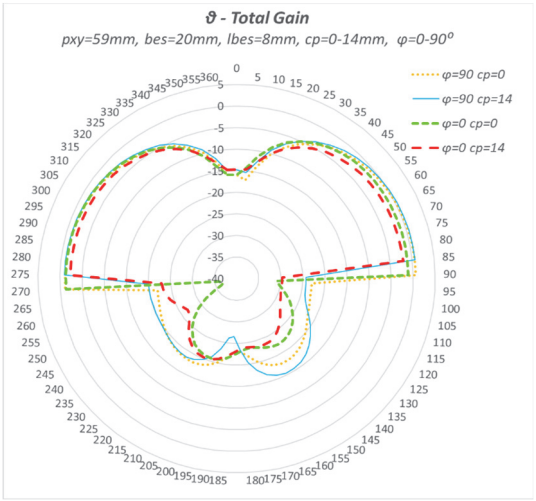

Figure 19 θ - Max_Gain (dB) Radiation Pattern graphs for *pxy* = 59 mm, *bes* = 20 mm, *lbes* = 8 mm, *dxy* = 30 mm, *cp* = 0 and 14 mm, φ = 0° and 90°

Table 4 Dimensions parameters of the used square patch antennas

Ant. Num	*cp* / mm	*pxy* / mm	*bes* / mm	*lbes* / mm
1	0	58	25	5
2	17	58	25	5
3	0	58	25	7
4	13	58	25	7
5	0	59	20	8
6	14	59	20	8

Gain and HPBW values obtained in HFSS and CST of antennas whose parameters are given in Tab. 4 are given in Tab. 5.

Table 5 Comparison of Gain and HPBW results obtained by HFSS and CST

Ant. Num	Gain / dB		HPBW / °	
	HFSS	CST	HFSS	CST
1	0,308	0,009	55,05	54,50
2	0,748	0,721	49,46	55,50
3	0,029	–0,126	55,12	54,60
4	0,211	0,698	54,41	54,90
5	0,559	–0,597	52,42	54,50
6	0,945	0,645	50,04	54,70

In the first antenna analysis, when the co-planar structure was added to the antenna, the gain value was enhanced from 0,308 dB to 0,748 dB. In the second antenna analysis, only the lbes parameter was changed from 5 mm to 7 mm. A 17 mm wide co-planar structure was added to this antenna and the antenna gain was enhanced from 0,029 dB to 0,211 dB. Finally, when the 13mm co-planar structure was added to the 3rd Antenna, the gain value improved from 0,559 dB to 0,945 dB. HPBW values changed from 55,05° to 49,46°, from 55,12° to 54,41° and from 52,42° to 50,04° when examined in the same order at HFSS simulation results.

4 CONCLUSION

In this study, for 3 different square patch antenna sizes, by changing the *cp* variable parametrically at 1 mm intervals, Maximum Gain values in different directions and Half Power Beam Width values were obtained, and the results are shown in tables and graphs.

When the results of HFSS were examined, it was determined that the co-planar structure enhanced the gain of the 1st antenna by 0,440 dB, the gain of the 2nd antenna by 0,182 dB and the gain of the 3rd antenna by 0,109 dB.

According to the CST simulation results, the gain was enhanced at the first antenna by 0,712 dB, the second antenna by 0,824 dB and the third antenna by 1,27 dB.

According to this, it is observed that there are improvements for all values where the gain is maximum. It has been concluded that the co-planar frame added to the antenna has a positive effect on the directionality of the antenna. Sudden power value drops normally observed at 90° and 270° angles shifted to 85° and 275° angles. Accordingly, it can be said that the coplanar structure added increases the directivity of the antenna.

Another measurement performed in this study was the determination of the Half Power Beam Width (HPBW). Opposite of the gain improvement, results showing that the Half Power Beam Width mostly decreased, and directionality generally increased were obtained.

As can be seen from these results, it was observed that adding co-planar structure to the antenna had a significant positive effect on Maximum Gain, which was one of the antenna parameters, and there was a reduction in HPBW values contrary to the gain. The decrease in HPBW and the increase in the gain mean that the directionality of the antenna generally has increased.

5 REFERENCES

[1] Cui, Y., Wu, L., & Li, R. (2018). Bandwidth enhancement of a broadband dual-polarized antenna for 2G/3G/4G and IMT base stations. *IEEE Transactions on Antennas and Propagation*, *66*(12), 7368-7373. https://doi.org/10.1109/TAP.2018.2867046

[2] Omar, A. A., Naser, S., Hussein, M. I., Dib, N. I., & Rashad, M. W. (2017). Superformula-Based Compact UWB CPW-Fed-Patch Antenna With and Without Dual Frequency Notches. *Applied Computational Electromagnetics Society Journal*, *32*(11), 979-986.

[3] Rabbani, M. S. & Ghafouri-Shiraz, H. (2016). Improvement of microstrip patch antenna gain and bandwidth at 60 GHz and X bands for wireless applications.*IET microwaves, antennas & propagation*, *10*(11), 1167-1173, 2016. https://doi.org/10.1049/iet-map.2015.0672

[4] Dardeer, O. M., Elsadek, H., & Abdallah, E. A. (2018). CPW-FED multiband antenna for various wireless communications applications. *IEEE International Symposium on Antennas and Propagation & USNC/URSI National Radio Science Meeting*, 785-786. https://doi.org/10.1109/APUSNCURSINRSM.2018.8609003

[5] Barrou, O., El Amri, A., Reha, A., & Hammouch, N. (2018). Performance Comparison between FIT and MoM Based Solvers for Microstrip Patch Array Antennas with Conventional Geometries. *International Journal of Computer Engineering and Information Technology*, *10*, 220-226.

[6] Gözel, M., Kasar, Ö., & Kahriman, M. (2019). 868 MHz UHF bandında H-şeklinde katlanmış implant mikroşerit dipol anten tasarımı. *Dicle Üniversitesi Mühendislik Fakültesi Mühendislik Dergisi*, *10*, 797-806. https://doi.org/10.24012/dumf.445660

[7] Li, K. J., Du, C. Z., Jin, G. Y., Zhao, Z. L., Zheng, W. Q., & Yang, F. H. (2020). A Wideband CPW-fed Monopole Hexagon Antenna for UWB Applications. *International Conference on Microwave and Millimeter Wave Technology (ICMMT)*, 1-3. https://doi.org/10.1109/ICMMT49418.2020.9386765

[8] Naik, K. K. & Gopi, D. (2018). Flexible CPW-fed split-triangular shaped patch antenna for WiMAX applications. *Progress in Electromagnetics Research M*, *70*, 157-166.

[9] Tarbouch, M., El Amri, A., & Terchoune, H. (2018). Design, realization and measurements of compact dual-band CPW-fed patch antenna for 2.45/5.80 GHz RFID applications. *International Journal of Electrical and Computer Engineering*, *8*(1), 172-178. https://doi.org/10.11591/ijece.v8i1.pp172-178

[10] Tiwari, R., Yogi, L., Bagwari, A., & Kushwah,V. S. (2019). Design and Performance Analysis of a Triple Band Micro-Strip Patch Antenna with CPW-Fed. *IJ Wireless and Microwave Technologies*, *9*, 36-42. https://doi.org/10.5815/ijwmt.2019.01.04

[11] Dastranj, A. & Abiri, H. (2010). Bandwidth enhancement of printed E-shaped slot antennas fed by CPW and microstrip line. *IEEE Transactions on Antennas and Propagation*, *58*(4), 1402-1407. https://doi.org/10.1109/TAP.2010.2041164

[12] Schandy, J., Steinfeld, L., Rodríguez, B., González, J. P., & Silveira, F. (2019). Enhancing parasitic interference directional antennas with multiple director elements. *Wireless Communications and Mobile Computing.* https://doi.org/10.1155/2019/7546785

[13] Da Xu, K., Xu, H., Liu, Y., Li, J., & Liu, Q. H. (2018). Microstrip patch antennas with multiple parasitic patches and shorting vias for bandwidth enhancement. *IEEE Access*, *6*, 11624-11633. https://www.doi.org/10.1109/ACCESS.2018.2794962

[14] Asaadi, M. & Sebak,A. (2017). Gain and bandwidth enhancement of 2 × 2 square dense dielectric patch antenna array using a holey superstrate. *IEEE Antennas and Wireless Propagation Letters*, *16*, 1808-1811. https://doi.org/10.1109/LAWP.2017.2679698

[15] Genc, A., Basyigit, I. B., Colak, B., & Helhel, S. (2018). Investigation of the characteristics of low-cost and lightweight horn array antennas with novel monolithic waveguide feeding networks. *AEU-International Journal of Electronics and Communications*, *89*, 15-23. https://doi.org/10.1016/j.aeue.2018.03.024

[16] Tawfeeq, N. N. (2017). Size reduction and gain enhancement of a microstrip antenna using partially defected ground structure and circular/cross slots. *International Journal of Electrical and Computer Engineering*, *7*, 894-898. https://doi.org/10.11591/ijece.v7i2.pp894-898

[17] Kawdungta, S., Jaibanauem, P., Pongga, R., & Phongcharoenpanich, C. (2017). Superstrate-integrated switchable beam rectangular microstrip antenna for gain enhancement. *Radioengineering*, *26*, 430-437. https://doi.org/10.13164/re.2017.0430

[18] Tiwari, R., Bagwari, A., & Kushwah, V. S. (2020). Parameter improvement of micro strip patch antennas using various techniques: A review. *Materials Today: Proceedings*, *29*, 492-500.

[19] Balanis, C. A. (2015). *Antenna theory: analysis and design*. John wiley & sons.

[20] Garg, R., Bhartia, P., Bahl, I. J., & Ittipiboon, A. (2001). *Microstrip antenna design handbook*. Artech house.

Contact information:

Orhan ARMAGAN, Instructor, PhD Student
(Corresponding author)
Isparta University of Applied Sciences,
Yalvaç Vocational School of Technical Sciences,
ISUBU-Yalvac Teknik Bilimler MYO - Yalvaç/Isparta
E-mail: orhanarmagan@isparta.edu.tr

Mesud KAHRİMAN, Associate Professor
Suleyman Demirel University Electronic and Communication Eng.,
Suleyman Demirel University Müh. Fakultesi - Isparta
E-mail: mesudkahriman@sdu.edu.tr